A Digital Hygrometer

HIROMI SHIMIZU, HIROKI MATSUMOTO, STUDENT MEMBER, IEEE, MASAHIRO ASAKURA, AND KENZO WATANABE, SENIOR MEMBER, IEEE

Abstract—**A digital hygrometer using a polyimide capacitive humidity sensor is developed. The capacitance change of the sensor due to adsorption of water vapor in the atmosphere is detected by a switched-capacitor digital capacitance bridge controlled by a one-chip microcomputer and is displayed as relative humidity with 0.1-percent resolution. The accuracy of the hygrometer calibrated by a two-point method is solely determined by the temperature dependence and the long-term drift of the dielectric sensitivity of the sensor and is estimated to be 2 percent.**

I. Introduction

A HAIR EXPANDS with humidity. This well-known physical phenomenon has been widely used as a hygrometer in daily life, but is not applicable to automatic humidity control of industrial, agricultural, and our living environments because it fails to provide an electrical signal. Among many electronic humidity sensors now being developed [1], a conductive-type sensor using a metal oxide or a ceramic and a capacitive-type sensor using a polymer film are promising candidates for low-cost mass production. The conductive sensors tolerate a high temperature environment, but suffer from a large temperature dependence and their sensitivity to pollution [2]–[4]. Therefore, the capacitive type seems preferable for accurate and stable humidity measurement at room temperature.

Typical hygroscopic materials used so far for sensing moisture in capacitive sensors are lithium-fluoride [5], cellulose acetate [6], and cellulose acetate butyrate [7]. While these hydrophilic films offer high sensitivity, their dielectric constants are sensitive to temperature and their capacitance change with humidity is highly nonlinear because of their nonuniform adsorption isotherm. Compared with them, the "dielectric sensitivity", i.e., the relative absorption of water vapor, of polyimide is rather small, but is much less sensitive to both temperature and thickness [8], [9]. In addition, good linearity can be expected between the bulk capacitance and relative humidity (RH) [10], [11]. Based on these predecessors' works, we have developed a linear humidity sensor. Its configuration and characteristics are described in the next section.

The capacitance change of the sensor due to RH is small compared with its offset capacitance. Therefore, accurate detection of RH and converting it to a microprocessor compatible signal require a capacitance bridge followed by an analog-to-digital (A/D) converter. Building such an interface using off-the-shelf components is possible, but is impractical from the viewpoint of the yield and the performance/price ratio. To accomplish the same function with a much simpler circuit and with an eye toward the possibility of on-chip signal conditioning, the digital capacitance bridge is developed based on a switched-capacitor charge-balancing A/D converter [12]. The digital circuitry for controlling this capacitance bridge can be easily implemented using standard logic gates, but a one-chip 8-bit microcomputer is used instead to accommodate other functions. This microcomputer-controlled interface is described in Section III.

Although the capacitance of the sensor changes linearly with RH, its offset capacitance and sensitivity differ from device to device. Therefore, two-point calibration is necessary for direct reading of RH. The calibration procedure and the overall performance of the digital hygrometer are discussed in Section IV. The paper concludes in Section V with the brief summary and the future work.

II. Humidity Sensor

The humidity sensor consists of a polyimide capacitor fabricated on a silicon substrate. The use of a silicon as a substrate offers the possibility of integrating the signal processing circuit and thus developing a "smart sensor". The fabrication procedure is as follows: First, Au is evaporated onto one surface of a 0.001 Ω-cm, n-type Si wafer 350 μm thick and is sintered at 650°C for 10 min to make the contact ohmic. After removing a SiO_2 layer on the other surface by chemical etching, the polyimide is spun onto a Si surface at 3000 rpm for 30 s. The polyimide film is prebaked at 200°C for 1 h and then cured at 350°C for 1 h. The hygroscopic film thus fabricated is typically 1.5 μm thick. Then, Au is evaporated onto the film through a metal mask to form a moisture-permeable, comb-like electrode. The thickness is typically 500 Å. A thin polyimide film less than 1 μm thick is again coated all over the surface, except the bonding pads, by dipping to protect the hygroscopic film from mechanical damage in the subsequent bonding and packaging process. This wafer is then scribed into chips measuring 8 mm × 12 mm. The configuration of the humidity sensor thus fabricated is shown in Fig. 1. Finally, each chip is mounted in a perforated metal header through which the sensor is exposed to the atmosphere.

Manuscript received October 15, 1987.

H. Shimizu and M. Asakura are with the Research and Development Division, Kurabe Industrial Co. Ltd., Kamimura, Hamana 432, Japan.

H. Matsumoto and K. Watanabe are with the Research Institute of Electronics, Shizuoka University, Hamamatsu 432, Japan.

IEEE Log Number 8820526.

0018-9456/88/0600-0300$01.00 © 1988 IEEE

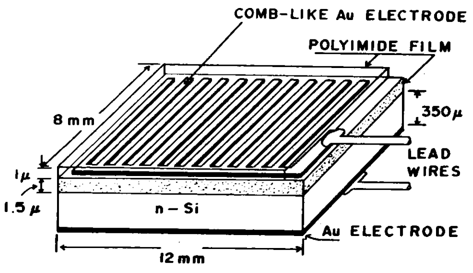

Fig. 1. The structure of the humidity sensor.

The bulk capacitance between the upper/comb-like and lower electrodes was measured over a humidity cycle from 20- to 90-percent RH and a temperature range from 15°C to 35°C. The accuracy of the reference hygrometer attached to the humidity-controlled environmental chamber is 3 percent. A commercially available four-terminal-pair bridge[1] was used for the capacitance measurement over the frequency range from 200 Hz to 500 kHz. Typical results measured at 10-kHz frequency are plotted in Fig. 2. No hysteresis was observed. As expected, a good linearity with a nonlinearity error of less than 0.2-percent and small temperature-dependence less than 0.1-percent RH/°C can be seen. The positive temperature coefficient is considered due to the thermal expansion of the film which allows more water to permeate the film. The dielectric sensitivity defined as the relative change in the capacitance for a unit change in RH is 3100 ppm, which is a typical value of the polyimide film cured at 300°C [10]. The capacitance decreases slightly with the increase in measurement frequency while keeping the sensitivity and the linearity constant [9]. The response time for the step change from 20- to 90-percent RH was about 5 s and that for the reverse change was about 7 s. These results indicate that the comb-like electrode is permeable to moisture and thus the response time is determined solely by diffusion through the film thickness.

Figure 3 shows the long-term stability tested for 8 weeks in various environments. During the first week of accelerated aging at 40°C and 90-percent RH, the sensor exhibited a rapid increase in the capacitance until it settled down to the steady-state value. The steady-state capacitance increases slightly when the sensor is exposed to a hot and wet atmosphere for a long period and decreases slightly when exposed to a hot and dry atmosphere for a long period. The fluctuation is, however, less than 2-percent RH. Therefore, the present sensor has proven its capacity for accurate and reliable RH measurement in the ordinary environments encountered in our daily life.

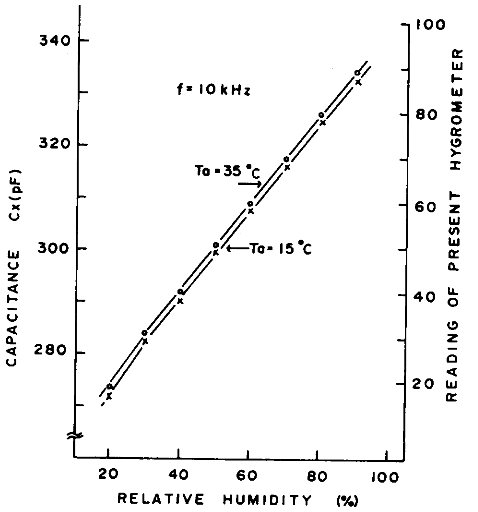

Fig. 2. The sensor capacitance C_X versus relative humidity (RH).

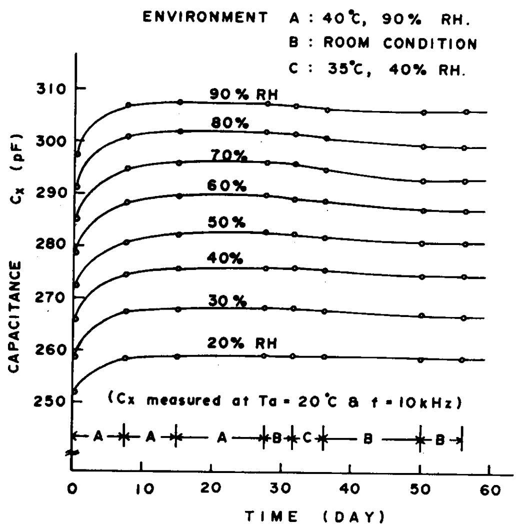

Fig. 3. The capacitance change of the sensor observed in the long-term test.

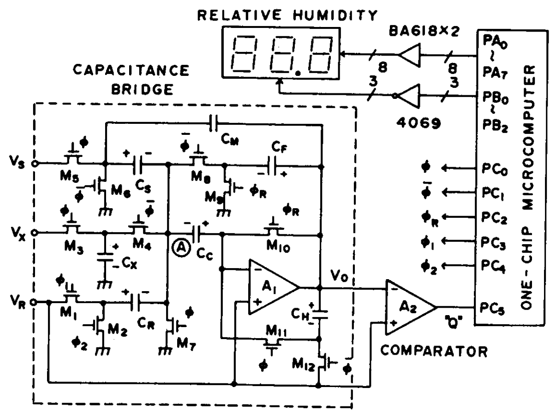

Fig. 4. The circuit diagram of the digital hygrometer.

III. Hygrometer Configuration

The whole circuit diagram of the digital hygrometer is shown in Fig. 4. It comprises three main blocks; the humidity sensor represented by C_X, the interface consisting of the capacitance bridge and the comparator A_2, and the one-chip 8-bit microcomputer. The humidity sensor has, in fact, the resistive component which should be connected in parallel with C_X. Because of the high volume-resistivity of polyimide, however, this parallel resistance is large enough to be neglected.

In the bridge, C_S is a standard capacitor to which C_X is compared. The difference between them is encoded into an n-bit binary number with reference to C_R. The capacitor C_F incorporated into the feedback path of op-amp A_1

[1]HP Model, 4275A, Multifrequency LCR Meter.

corresponds to a detection arm of a conventional bridge. Capacitors C_C and C_H are incorporated so that the balance operation of the bridge is insensitive to the offset voltage and the finite open-loop gain of op-amp A_1 [13]. ϕ and $\overline{\phi}$ are the nonoverlapping two phase clocks for driving the analog switches involved in the bridge. Capacitor C_M is incorporated to prevent the spikes which would otherwise be generated by op-amp A_1 in the nonoverlapping period [14]. This capacitor has, however, no effect upon the bridge balance operation and is thus neglected henceforth.

Comparator A_2 compares the bridge output V_o with the reference voltage V_R, to inform the microcomputer of the present state of the bridge. Depending on the comparator output "Q", the microcomputer produces clock signals ϕ_1 and ϕ_2 which control switches M_1 and M_2, respectively, to balance the bridge digitally. The logic expressions for $\phi_1(n)$ and $\phi_2(n)$ in the nth cycle of the two phase clock are given by

$$\phi_1(n) = \overline{Q(n-1)} + \phi(n) \tag{1}$$

$$\phi_2(n) = Q(n-1) \cdot \overline{\phi(n)} \tag{2}$$

where $Q(n-1)$ denotes the logic level of the comparator output in the preceding clock cycle. The operation of the interface will now be described in more detail.

The timing diagram of the clock signals and the output voltage waveform of the capacitance bridge are depicted in Fig. 5. To begin with, the microcomputer outputs a reset pulse ϕ_R in synchronism with the ϕ clock signal to initialize the bridge. The output voltage of op-amp A_1 is V_R. Thus, in this reset phase, C_C and C_F are charged to V_R, while C_X, C_S, and C_R are charged to V_X, V_S, and V_R, respectively, with the polarity indicated in Fig. 4. Because C_C is charged to V_R, the node A can be regarded as the virtual ground terminal of op-amp A_1 [13]. Let us assume that the comparator output in the previous measurement cycle is "1". Then, in the next $\overline{\phi}$ phase, ϕ_2 becomes "1" and the charge $Q_R = C_R V_R$ stored in C_R is transferred, (together with the charges $Q_X = C_X V_X$ and $Q_S = C_S V_S$ stored in C_X and C_S, respectively) into C_F to charge it with the polarity indicated. The net charge accumulated in C_F by this process is

$$Q_{acc} = Q_R + Q_S - Q_X. \tag{3}$$

Since the dc voltages V_R, V_S, and V_X are chosen such that Q_{acc} be positive, the charge accumulation in this phase increases the bridge output V_o by Q_{acc}/C_F and the comparator output "Q" becomes "0". In the ϕ phase of the next cycle, C_R, C_S, and C_X are charged again to their own voltages. In the next $\overline{\phi}$ phase, C_X and C_S are discharged to transfer their charges to C_F, while C_R remains charged because the switch M_2 is kept "off". Since the voltages V_X and V_S are chosen such that $Q_X > Q_S$, the charge

$$Q_{ext} = Q_X - Q_S \tag{4}$$

is extracted from C_F by this process and the output voltage of the bridge decreases by Q_{ext}/C_F, as shown in Fig. 5. This charge extraction continues until the comparator output "Q" becomes "1" and the charge Q_{acc} is accumulated again into C_F. Repeating the above process of the charge accumulation and extraction for N cycles of the two-phase clock until the next reset pulse ϕ_R initializes the bridge, the microcomputer counts the number of times the charge Q_{ext} is extracted.

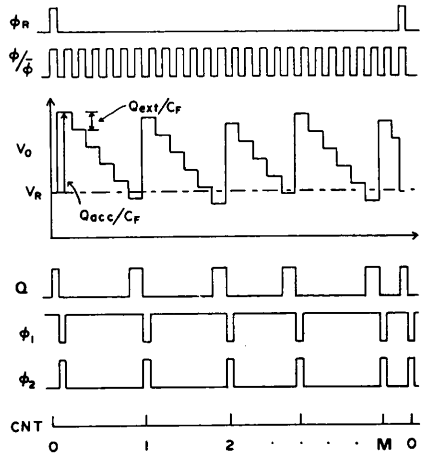

Fig. 5. Timing diagram and the output voltage waveform of the capacitance bridge.

Let the count be M. Then, the total charge accumulated into C_F is MQ_{acc}, while that extracted from C_F is $(N - M)Q_{ext}$. Therefore, the bridge output $V_o(N)$ at the end of one measurement cycle is

$$V_o(N) = V_R + [MQ_R - N(Q_X - Q_S)]/C_F. \tag{5}$$

Referring to Fig. 5, one notices that the bridge output is always in the range from $V_R - Q_{ext}/C_F$ to $V_R + Q_{acc}/C_F$. Thus, we can obtain the relation

$$M/N - (Q_X - Q_S)/Q_R < 1/N = 1 \text{ LSB}. \tag{6}$$

The capacitance C_X of the humidity sensor can be represented as

$$C_X = C_o(1 + S_d \cdot \text{RH}) \tag{7}$$

where C_o is the offset capacitance and S_d denotes the "dielectric sensitivity" of the sensor. Adjusting V_S and V_R such that $C_o V_X = C_S V_S$ and $C_o V_X S_d = C_R V_R$ hold, respectively, and setting $N = 2^n$, one can obtain, from (6), the n-bit binary representation of RH

$$\text{RH} = M/2^n = m_1 2^{-1} + m_2 2^{-2} + \cdots + m_n 2^{-n}. \tag{8}$$

Figure 6 shows the flowchart of the control subroutine. The subroutine uses the "DE" pair register for counting the number N of the two-phase clock cycle and the "HL" pair register for counting M. After resetting these registers, the program enters the $\overline{\phi}$-state. In this state, the ϕ, ϕ_1, and ϕ_R clocks are first reset to "0", and then, after 5.4 μs, $\overline{\phi}$ and ϕ_2, if "Q" = "1", clocks are set to "1" and outputted to the bridge from port C. The $\overline{\phi}$ clock lasts for 22.5 μs until it is reset to "0" in the ϕ-state. Incrementing the "DE" register and then sensing the output level "Q" of comparator A_2, the program completes the operation in the $\overline{\phi}$-state.

In the ϕ-state, the program first resets ϕ, ϕ_1, and ϕ_2 clocks. Thus, all the clocks are "off" until the ϕ and ϕ_1

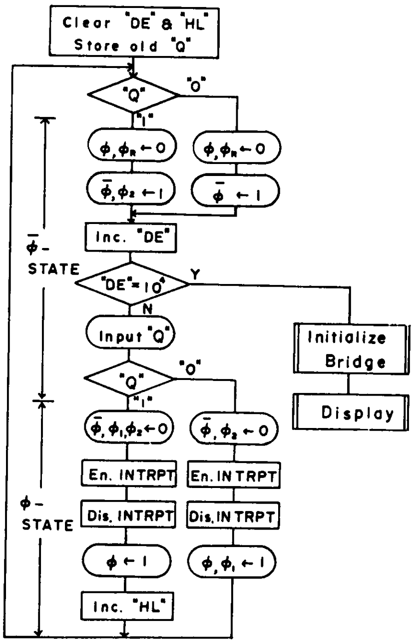

Fig. 6. The flow chart of the bridge control program.

clocks are set to "1". In this period, the subroutine accepts the interrupt request from the event timer which, accommodated in the microcomputer, produces the "digit select signal" every 6.6 ms for a dynamic display of RH. The time required for processing the interrupt request is 38.5 μs. If the interrupt is absent, the time elapsed before the ϕ clock is set to "1" is 8.7 μs. The ϕ clock lasts for 13 μs until it is reset to "0" in the $\bar{\phi}$-state. Incrementing the "HL" register if "Q" = "1", the program completes the operation in the ϕ-state.

In this subroutine, N is set to 10^4. Therefore, the program repeats the operation in the $\bar{\phi}$- and ϕ-states 10^4 times (the ϕ-state operation in the last cycle is included in the "Bridge initialize" subroutine). The time required for one measurement cycle is about 470 ms, although it depends on the number of the interrupt request. The count M stored in the "HL" register is divided by 10, converted to the 3-digit BCD, and displayed as the relative humidity with 0.1-percent resolution by the "display" subroutine.

IV. Calibration and Accuracy

Although the humidity sensor is fabricated using IC compatible technologies, its offset capacitance and sensitivity differ from chip to chip. In addition, the interface circuit includes many nonideal factors such as the offset voltage V_{os1} and the finite open-loop gain A_1 of op-amp A_1, the offset voltage V_{os2} of comparator A_2, the parasitic capacitance between each circuit node and ground, and the clock feedthrough involved in analog switches. In this section, the effect of these nonideal factors upon the measurement accuracy is evaluated to establish the calibration procedure and also to have an insight into the feasibility of the on-chip interface.

Figure 7 shows the interface circuit including the nonideal factors. Taking these deleterious factors into account, one can derive the following expressions for the charges accumulated in and extracted from C_F:

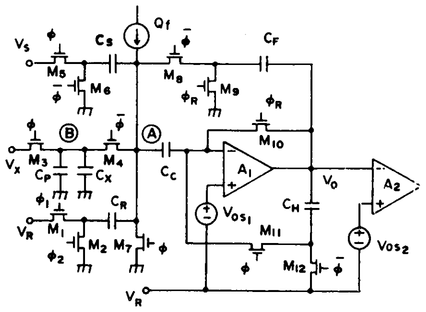

Fig. 7. The interface circuit, including the nonideal elements.

$$Q'_{\rm acc} = (C_R V_R + C_S V_S - C'_X V_X)/(1 + \epsilon) \quad (9)$$

$$Q'_{\rm ext} = (C'_X V_X - C_S V_S)/(1 + \epsilon) \quad (10)$$

where

$$\epsilon = [1 + (C'_X + C_S + C_R)/C_F]/A_1 \quad (11)$$

$$C'_X = C_X + C_P + Q_f/V_X \quad (12)$$

Q_f is the clock feedthrough charge injected into node A, and C_p is the parasitic capacitance between node B and ground. Parasitic capacitances other than C_p have no effect upon the charge transfer. The denominator $1 + \epsilon$ of (9) and (10) indicates the reduction in the charge transfer efficiency due to the finite open-loop gain A_1 of op-amp A_1. The final bridge output $V'_o(N)$ is then given by

$$V'_o(N) = V_R + V_{os1} + [MQ'_{\rm acc} - (N - M)Q'_{\rm ext}]/C_F. \quad (13)$$

Since $V'_o(N)$ is in the range

$$V_R + V_{os2} - Q'_{\rm ext}/C_F < V'_o(N) < V_R + V_{os2} + Q'_{\rm acc}/C_F. \quad (14)$$

We have, after a little manipulation

$$(Q_{os} - Q'_{\rm ext})/(NQ'_R) < M/N - Q'_{\rm ext}/Q'_R < (Q_{os} + Q'_{\rm acc})/(NQ'_R) \quad (15)$$

where

$$Q_{os} = C_F(V_{os2} - V_{os1}) \quad (16)$$

$$Q'_R = C_R V_R/(1 + \epsilon). \quad (17)$$

Since N is very large, 10^4 in practice, the effect of the offset voltages upon the measurement accuracy is negligible. The finite gain A_1 does not disturb the bridge balance either, because the reduction of the charge transfer efficiency is common to both $Q'_{\rm acc}$ and $Q'_{\rm ext}$. Therefore, the interface measures digitally

$$m = M/N = [(C_o + C_o S_d {\rm RH} + C_p)V_X + Q_f - C_S V_S]/(C_R V_R). \quad (18)$$

The direct reading of RH on the display requires

$$(C_o + C_p)V_X + Q_f = C_S V_S \tag{19}$$

$$C_o S_d V_X = C_R V_R. \tag{20}$$

To meet the above conditions for the offset cancellation and the sensitivity adjustment, two-point calibration is obliged; first, the reading m_1 when the humidity sensor is exposed to the atmosphere of some reference humidity RH_1 is noted. Then, expose the sensor to the atmosphere of different humidity RH_2. Watching the reading m_2, adjust the reference voltage V_R such that $m_2 - m_1$ coincides with RH_2-RH_1. This establishes the sensitivity condition (20). Next, adjust the voltage V_S such that m_2 coincides with RH_2. This establishes the offset cancellation condition (19).

The readings of the hygrometer thus calibrated are indicated on the right-hand ordinate of Fig. 2 for the humidity cycle from 20 to 90 percent. Because the calibration eliminates the errors caused by the nonideal factors involved in the interface and compensates the deviations of the offset capacitance and the sensitivity of the humidity sensor, the error of this hygrometer is solely determined by the temperature dependence and the long-term drift of the sensor and is estimated, from data in Figs. 2 and 3, to be less than 2 percent.

V. Conclusions

A digital hygrometer using the polyimide capacitive humidity sensor is described. The switched-capacitor interface for detecting the capacitive change of the sensor and converting it into the digital number is very simple and requires no component matching and trimming. Therefore, a low cost and compact "smart humidity sensor" can be realized by integrating the hygroscopic film and the interface circuit onto a single Si chip.

The accuracy of the present hygrometer is limited to 2 percent by the temperature dependence and the long-term drift of the humidity sensor. The temperature compensation can be easily accomplished by the software because the one-chip microcomputer accommodates the analog-to-digital converter available for converting the voltage across a temperature sensor such as a junction diode or a thermister into the digital number. This will allow the indication of the temperature-humidity index as well as the improvement of the RH measurement accuracy.

References

[1] K. Schurer, "Humidity sensors," *J. A*, vol. 22, pp. 156-161, Mar. 1981.

[2] R. T. Johnson, Jr. and R. M. Biefeld, "Ionic conductivity of Li_5AlO_4 and Li_5GaO_4 in moist air environments: Potential humidity sensors," *Mat. Res. Bull.*, vol. 14, pp. 537-542, Apr. 1979.

[3] P. Wiedijk, "Flat-based water vapour sensor of the phosphorous pentoxide type," *J. Phys. E: Sci. Instrum.*, vol. 13, pp. 993-994, Sept. 1980.

[4] T. Usui, A. Asada, and Y. Inose, "Limiting current type multifunctional sensor: Oxygen-humidity sensor," *IEEE Instrum. Meas. Tech. Conf. Proc.*, pp. 305-310, 1987.

[5] L. C. Yang, "Developments in moisture sensors," *Meas. Control*, vol. 15, pp. 98-108, Feb. 1981.

[6] "Capacitive humidity sensor," Tech. Inform. 063, Philips Nederland B. V., Eindhoven, The Netherlands, 1980.

[7] P. E. Thoma, J. O. Colla, and R. Stewart, "A capacitive humidity-sensing transducer," *IEEE Trans. Components, Hybrids, Manufact. Technol.*, vol. CHMT-2, pp. 321-323, Sept. 1979.

[8] E. Sacher and J. R. Susko, "Water permeation of polymer films: III, High temperature polyimides," *J. Appl. Polym. Sci.*, vol. 26, p. 679, 1981.

[9] P. J. Schubelt and J. H. Nevin, "A polyimide-based capacitive humidity sensor," *IEEE Trans. Electron Dev.*, vol. ED-32, pp. 1220-1223, July 1985.

[10] D. D. Denton, S. D. Senturia, E. S. Anolick, and D. Scheider, "Fundamental issues in the design of polymeric capacitive moisture sensors," in *Int. Conf. Solid-State Sensors Actuators, Dig. Tech. Papers*, pp. 202-205, 1985.

[11] M. C. Glenn and J. A. Schuetz, "An IC compatible polymer humidity sensor," in *Int. Conf. Solid-State Sensors Actuators, Dig. Tech. Papers*, pp. 217-220, 1985.

[12] H. Matsumoto, H. Shimizu, and K. Watanabe, "A switched-capacitor charge-balancing analog-to-digital converter," in *Proc. IEEE Instrum. Meas. Tech. Conf.*, 1987, pp. 110-114.

[13] K. Nagaraj, J. Vlach, T. R. Viswanathan, and K. Singhal, "Switched-capacitor integrator with reduced sensitivity to amplifier gain," *Electron. Lett.*, vol. 22, pp. 1103-1105, 1986.

[14] H. Matsumoto and K. Watanabe, "Spike-free switched-capacitor circuits," *Electron. Lett.*, vol. 23, pp. 428-429, Apr. 1987.